

A Newly designed cell-permeable SNARF derivative as an effective intracellular pH indicator

by

Eiji Nakata^{1*}, Yoshihiro Yukimachi², Yoshijiyo Nazumi², Yoshihiro Uto¹, Hitoshi Hori¹

Abstract

SNARF is one of the most commonly used pH indicators for biological applications, owing to its unique fluorescent characteristics. For intracellular applications, esterase-substrate derivatives of SNARF, such as acetate or acetoxymethyl esters, have been employed previously as a generally accepted strategy to increase cell permeability. Unfortunately such cell-permeable SNARF derivatives retain significant fluorescence in aqueous solution, a property which results in a low signal-to-noise ratio. This in turn can lead to incorrect intracellular pH measurements. Here we describe UTX-40, a newly designed SNARF derivative that successfully addresses these problems. In aqueous solution, UTX-40 is devoid of fluorescence before ester hydrolysis because it exists in aqueous environment as nano-scaled aggregates. As UTX-40 is converted into SNARF by enzymatic hydrolysis inside the cell, the aggregates become diffused and monomeric SNARF displays its characteristic fluorescent properties. The results of our studies reported in this communication demonstrate clearly the benefits of UTX-40 as an intracellular pH indicator. Since intracellular localized fluorescence was observed without cell-washing, the efficient uptake of intracellular fluorescence was confirmed. In addition, the actual intracellular pH and changes in intracellular pH caused by drug addition were monitored. The low background noise produced by UTX-40 is a property of this new pH probe that should be particularly advantageous for in vivo usage because, for this application, it is difficult to wash out the redundant probe.

Keywords: Fluorescent pH indicator, bio-imaging, intracellular pH measurement, SNARF

The dynamics of intracellular pH (pH_i) is crucial for understanding the mechanisms of regulation of many physiological functions of the cell.¹ Among the several methods available to

determine pH_i , optical methods have various advantages including rapid response time, high signal-to-noise ratio, noninvasiveness, and excellent pH sensitivity.² Various types of fluorescent pH_i indicators have been developed,³ and some have been successfully applied to monitoring changes in pH_i .⁴ Using these indicators, the role of fluctuations in pH_i during the course of endocytic events has been examined.⁵

¹ Division of Bioinformatics Engineering, Department of Life System, Institute of Technology and Science, Graduate School of the University of Tokushima

² Graduate School of Advanced Technology and Science, The University of Tokushima

* The University of Tokushima, 2-1 Minamijosanjima, Tokushima, 770-8506, Japan

SNARF (seminaphthorhodafluor) is one of the most commonly used pH indicators, because of its unique fluorescent characteristics. These include to be excited by visible light, dual-emission properties for ratiometric measurement and a neutral pK_a region suitable for monitoring physiological pH ranges.⁶ In aqueous solution, the phenolic substituent of SNARF is critical for its dual-emission properties in that an equilibrium exists between the acidic phenol form with a λ_{em} of 583 nm (λ_{max} of 544 nm) (written as SNARF(A)) and the basic phenolate form with a λ_{em} of 627 nm (λ_{max} of 573 nm) (written as SNARF(B)). Thus, the pH is calculated by the ratio of SNARF(A) and SNARF(B). An additional equilibrium involves formation of a colorless and

nonfluorescent lactone, which is the dominant form of SNARF in nonpolar environments (written as SNARF(L)).^{6,7}

To increase cell permeability, the phenolic group of SNARF is converted to esterase substrates such as acetate or acetoxymethyl ester derivatives.^{3a,7} However such cell-permeable SNARF derivatives retain fluorescence (λ_{em} of 583nm) characteristic of SNARF(A) in aqueous solution. This may result in a low signal-to-noise ratio if the media have fluorescence or to incorrect pH measurement if the protected SNARF remains inside the cell. Therefore, a SNARF derivative that is non-fluorescent before hydrolysis should have advantages for accurate pH monitoring.

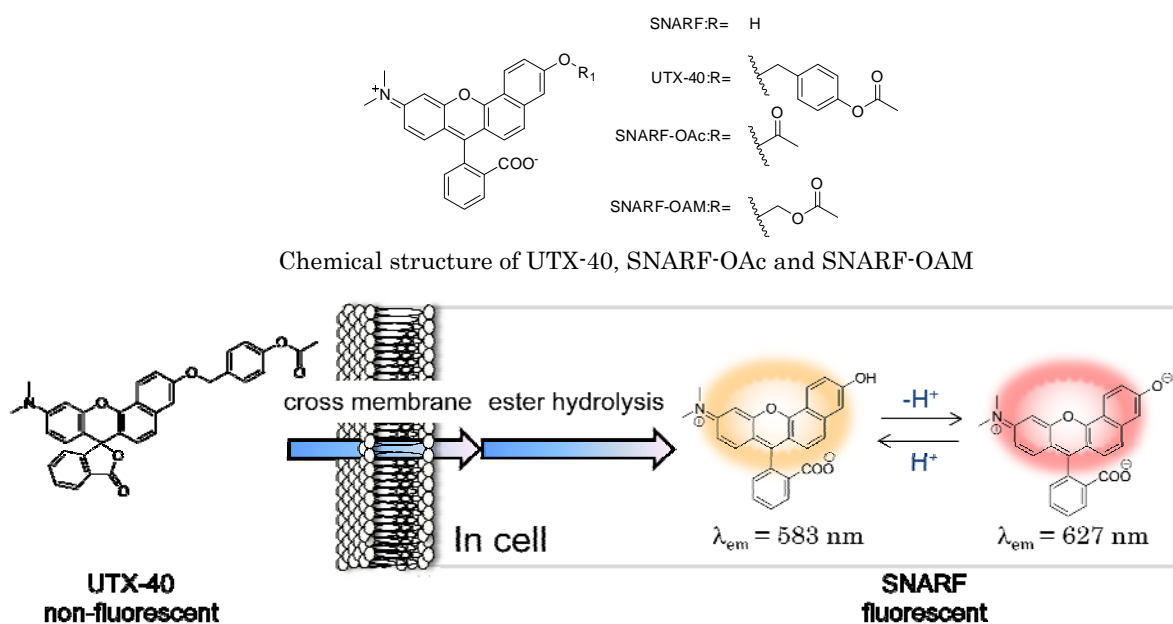


Fig. 1 Schematic illustration of UTX-40 activation by intracellular ester hydrolysis.

We recently reported non-fluorescent SNARF derivatives in which the phenolic substituents were protected by a benzyl group, because these compounds exist mainly as SNARF(L) in aqueous solution.⁸ These results prompted us to prepare a newly designed SNARF derivative UTX-40, which

emits fluorescence only after ester hydrolysis (Fig. 1). UTX-40 is comprised of a *p*-acetoxybenzyl moiety directly linked to SNARF through an ether linkage. SNARF-OAc and SNARF-OAM, the phenolic moieties of which were masked by acetyl and acetoxymethyl respectively, were also synthesized as

control compounds (details of the synthetic procedures for UTX-40, SNARF-OAc and SNARF-OAM are provided in the ESI).

Evaluation of the spectroscopic properties of these SNARF derivatives (Fig. 2a) and Table 1) revealed that SNARF-OAc and SNARF-OAM produced the distinctive absorption and fluorescent spectra of SNARF(A). On the other hand, 10 times smaller absorption peaks and very weak fluorescence were observed when UTX-40 was measured, indicating that UTX-40 was mainly in the form of SNARF(L). When compared to the brightness of SNARF(A), UTX-40 was almost 100 times less bright (1.1% of relative brightness) as shown in Table 1. In contrast, SNARF-OAM and SNARF-OAc display significant fluorescence, albeit with somewhat lower brightness (46% and 18% respectively). These properties were clearly confirmed under transilluminator observations (Fig. 2b)). Evaluation of the spectroscopic properties of these SNARF derivatives (Fig. 2a) and Table 1) revealed that SNARF-OAc and SNARF-OAM produced the distinctive absorption and fluorescent spectra of SNARF(A). On the other hand, 10 times smaller absorption peaks and very weak fluorescence were observed when UTX-40 was measured, indicating that UTX-40 was mainly in the form of SNARF(L). When compared to the brightness of SNARF(A), UTX-40 was almost 100 times less bright (1.1% of relative brightness) as shown in Table 1. In contrast, SNARF-OAM and SNARF-OAc display significant fluorescence, albeit with somewhat lower brightness (46% and 18% respectively). These properties were clearly confirmed under transilluminator observations (Fig. 2b)).

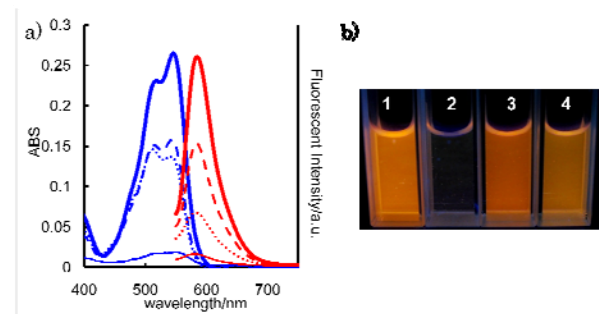


Fig. 2 a) Absorbance (blue) and fluorescence (red) spectra of SNARF (bold line), UTX-40 (plane line), SNARF-OAM (dash line) and SNARF-OAc (dot line) at pH 5.0. b) Photograph of SNARF(1), UTX-40(2), SNARF-OAM(3) and SNARF-OAc(4) at pH 5.0.

Table 1 Spectroscopic properties of SNARF derivatives used in this study.

Dye	$\lambda_{\text{ABS}} (\epsilon)^a$ (nm)(M ⁻¹ cm ⁻¹)	λ_{em}^b (nm)	Φ	Rel ^c
SNARF(pH5.0) ^d	515 (17700)	583	0.030	100%
	544 (21600)			
UTX-40	520 (1344.1)	581	0.005	1.1%
	559 (1383.3)			
SNARF-OAc	515 (18370)	581	0.0081	18%
	545 (17388)			
SNARF-OAM	515 (15092)	580	0.019	46%
	543 (15854)			

^a Measured in pH 5.0 10 mM acetate buffer. ^b Excited at 534 nm. ^c Rel (relative brightness) was calculated using the following equation. $\text{Rel}_{\text{sample}} = \epsilon \times \Phi / \epsilon_{\text{SNARF}} \times \Phi_{\text{SNARF}}^{\text{ref.6a}}$

Next, the behavior of these derivatives as esterase substrates was evaluated. Though all of these SNARF derivatives could be hydrolyzed by esterase, the spectroscopic behavior during ester hydrolysis was clearly different. When SNARF-OAM was treated with esterase at pH 7.5, a seesaw type of absorption spectral change with an isosbestic point (525 nm) was observed (Fig. 3b)). This indicated that the form of SNARF-OAM was converted from SNARF(A) to SNARF(B) by ester hydrolysis. A similar spectral change was observed during hydrolysis of SNARF-OAc with an isosbestic point at 510 nm (data not shown). However with

UTX-40, a simple incremental absorption change occurred. This indicated that UTX-40 was being converted from SNARF(L) to the quinoid form (SNARF(A) and SNARF(B)) during ester hydrolysis. Furthermore, the fluorescent spectral changes during hydrolysis agreed well with the results obtained from the absorption measurements (inset of Fig. 3). Dynamic light scattering (DLS) measurements of UTX-40 and SNARF-OAM before and after esterase treatment suggested the cause of these different spectroscopic properties.⁹ DLS intensity showed that the buffer solution of UTX-40 before esterase treatment consistently contained aggregates having a diameter of mean size 75.7 ± 7.7 nm, whereas negligible DLS intensity was obtained after treatment with esterase. On the other hand, in the case of SNARF-OAM, we did not observe DLS intensity either before or after treatment with esterase. This shows that SNARF-OAM existed as a monomer throughout the course of ester hydrolysis. These results suggest that the aggregates of UTX-40 make a hydrophobic environment by themselves, which induced the displacement of equilibrium toward SNARF(L). As UTX-40 is converted into SNARF by enzymatic hydrolysis, the aggregates become diffused and monomeric SNARF displays its fluorescent properties.

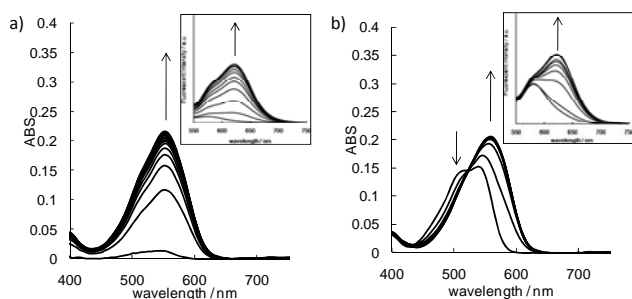


Fig. 3 Real time absorbance change via esterase-catalyzed ester hydrolysis at pH 7.5. a) UTX-40 and b) SNARF-OAM. (Inset) Fluorescence spectral change (excited at 534 nm)

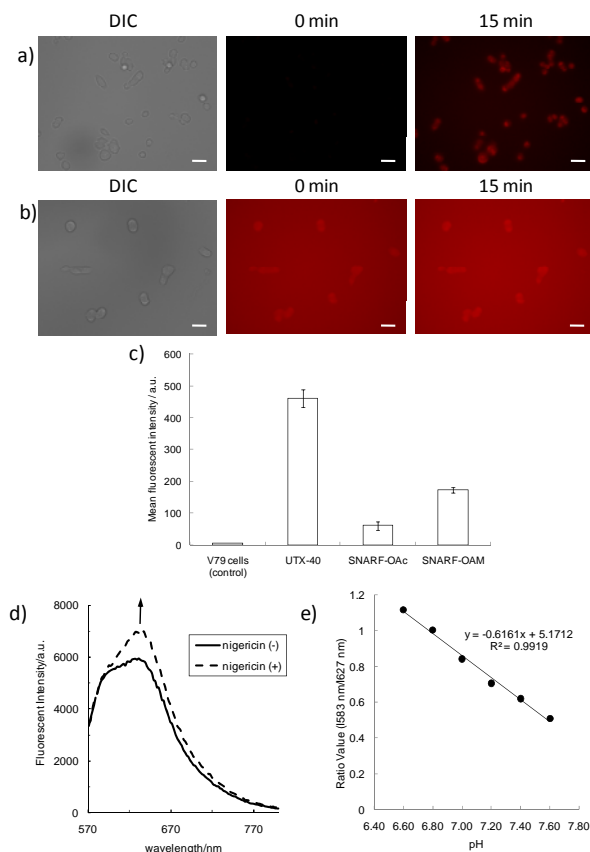


Fig. 4 Bright-field transmission and fluorescence images of V79 cells after addition of a) UTX-40 (10 μ M) or b) SNARF-OAM (10 μ M) to extracellular solution (EMEM). The scale bars (30 μ m) are shown in the photograph. c) Mean fluorescence intensity of SNARF into V79 cells analyzed by FACS (n = 4). d) Intracellular fluorescence spectra of SNARF measured by micro plate reader before (plane line) and after (dash line) addition Nigericin (10 μ g/ml) in PBS (pH 7.2). e) The standard curve with pH values to determine the intracellular pH.

Finally, the properties of the new derivatives as pH_i indicators were evaluated.¹⁰ The uptake of the SNARF-based fluorescent intensity inside V79 cells (Chinese hamster lung) was confirmed by fluorescent microscopic analysis. Immediately on addition of SNARF-OAM (Fig. 4b)) or SNARF-OAc (data not shown), a strong background signal from medium was observed. Therefore it was very difficult to distinguish between the inside and outside of the cell. However in the case of UTX-40 (Fig. 4a)), the medium was scarcely fluorescent under the same conditions, and only the uptake of the fluorescent

intensity inside the cell was observed after 15 min incubation.¹¹ This result strongly indicates the benefit of the UTX-40 in reducing the background noise before ester hydrolysis. In addition, the cellular uptake of the SNARF was quantitatively evaluated by flow cytometry analysis. As shown in Fig. 4c), the effective cellular uptake of SNARF was confirmed in the case of UTX-40 as compared to SNARF-OAc or SNARF-OAM. Furthermore, the actual pH_i values of V79 cells in PBS (pH 7.2) were determined using UTX-40. The fluorescent spectra of SNARF inside cells are shown Fig. 4d). The ratio values R ($= 583 \text{ nm} / 627 \text{ nm}$) were determined to be 0.81 ± 0.01 . According to a standard curve which was constructed by conventional methods (Fig. 4e))¹², an accurate pH_i was determined as 7.1, which is consistent with the commonly-known range of pH_i ¹³. After adding nigericin, serving as an ionophore to equilibrate pH_i and extracellular pH, the value of R became 0.72 ± 0.03 corresponding to a converted pH of 7.2 which is the value of extracellular pH. These results establish the superiority of UTX-40 as a pH_i indicator that has notable cell permeability and that is non-fluorescent before hydrolysis, properties that will greatly facilitate intracellular applications.

In conclusion, we have developed UTX-40 as a new SNARF-derived pH_i indicator which is notable for its efficient uptake and lack of fluorescence prior to cellular uptake, because it formed nonfluorescent aggregates in aqueous media. Efficient esterase hydrolysis leads to diffusion of the aggregates and to intracellular-localized fluorescence with low background fluorescence. The low background noise should be particularly advantageous for in vivo usage, because for this application there is difficulty in washing out the redundant probe. Therefore we envision further applications of in vivo usage of this

agent for pH monitoring inside the cell and drug screening applications that involve pH regulation inside the cell.

Acknowledgements

The authors thank Prof. Hiroshi Maezawa (University of Tokushima) for support of cellular experiments. The authors also thank Mr. Koji Matsuda (KEYENCE) for his support on the microscopic measurement, and Dr. Atsushi Tabata (University of Tokushima) for his help on the flow cytometry measurement. This work was supported by the 2009 Research Project of Faculty and School of Engineering, The University of Tokushima.

References and notes

1. J. Barber, D. L. Barber, M. P. Jacobson, *Physiol.*, 2007, **22**, 30. a) J. K. Willmann, N. V. Bruggen, L. M. Dinkelbuorg, S. S. Gambhir, *Nature Rev. Drug Discov.*, **2008**, **7**, 591. b) R.J. Hargreaves, *Clinical pharmacology & Therapeutics*, 2008, **83**, 349.
2. a) J. Han, K. Burgess, *Chem. Rev.*, ASAP. b) R. Bizzarri, M. Serresi, S. Luin, F. Beltram, *Anal. Bioanal. Chem.*, 2009, **393**, 1107. c) L. Lavis, R. T. Rains, *ACS Chem. Biol.* 2008, **3**, 142. d) K. Johnsson, N. Johnsson, *ACS Chem. Biol.* 2007, **2**, 31.
3. a) Y. Urano, D. Asanuma, Y. Hama, Y. Koyama, T. Barrett, M. Kamiya, T. Nagano, T. Watanabe, A. Hasegawa, P. L. Choyke, H. Kobayashi, *Nat. Med.*, 2009, **15**, 104. b) T. Ohmichi, Y. Kawanomoto, P. Wu, D. Miyoshi, H. Karimata, N. Sugimoto, *Biochemistry*, 2005, **44**, 7125. c) J. Han, A. Loudet, R. Barhoumi, R. C. Burghardt, K. Burgess, *J. Am. Chem. Soc.*, 2009, **131**, 1642. d) B. Tang, F. Yu, P. Li, L. Tong, X. Duan, T. Xie, X. Wang, *J. Am. Chem. Soc.*, 2009, **131**, 3016.
4. (a) J. G. Wann, Y. Hsu, C. Yang, C. Lin, D. W. Tai, J. Chen, C. Hsiao, C. Chen, *Nephrol. Dial. Transplant.*, 2007, **22**, 2613 (b) C. Nilsson, K. Kagedal, U. Johansson, K. Ollinger, *Methods in Cell Science.*, 2003, **25**: 185–194. (c) S. R. Sennoune, K. Bakunts, G. M. Martinez, J. L. Chua-Tuan, Y. Kebir, M. N. Attaya, R. Martinez-Zaguilan, *Am. J. Physiol. Cell. Physiol.*, 2004, **286**, C1443. (d) C. Nilsson, U. Johansson, A. Johansson, K. K. Ollinger, *Apoptosis*, 2006, **11**, 1149.
5. J. E. Whitaker, R. P. Haugland, F. G. Prendergast, *Anal. Biochem.*, 1991, **194**, 330.
6. R. P. Haugland, in *Handbook of Fluorescent Probes and Research Products*, Molecular Probes, Inc., Eugene, OR, 2002, 9th edn.

7. E. Nakata, Y. Yukimachi, H. Kariyazono, S. Im, C. Abe, Y. Uto, H. Maezawa, T. Hashimoto, Y. Okamoto, H. Hori, *Bioorg. Med. Chem.*, 2009, **17**, 6952.
8. Y. Takaoka, T. Sakamoto, S. Tsukiji, M. Narazaki, T. Matsuda, H. Tochio, M. Shirakawa, I. Hamachi, *Nat. Chem.*, 2009, **1**, 557.
9. According to absorption measurements, UTX-40 mainly formed SNARF(L) in medium with serum.
10. The localization of deprotected UTX-40 or SNARF-OAM, that is SNARF, was confirmed by a multistaining procedure (data not shown).
These experiments demonstrated that SNARF was localized mainly in mitochondria and cytosol. These results were consistent with previous reports (ref. 3a)).
11. a) J. A. Thomas, R. N. Buchsbaum, A. Zimniak, E. Racker, *Biochemistry*, 1979, **18**, 2210. b) J. Bond, J. Varley, *Cytometry*, 2005, **64A**, 43.
12. a) M. C. Brahimi-Horn, J. Pouyssegur, *FEBS Lett.* 2007, **581**, 3582. b) P. Swietach, R. D. Vaughan-Jones, A. L. Harris, *Cancer Metas. Rev.* 2007, **26**, 299.